SPACE ROBOTICS APPLICATION FOR LARGE SPACE STRUCTURES

Ijar M. Da Fonseca[+]
Space Mechanics and Control Division – DMC
National Institute for Space Research – INPE
Avenida dos Astronautas, 1758 – P.O. Box 515
12201-970 São Jose dos Campos, S.P., Brazil
E-mail: ijar@dem.inpe.br

Peter M. Bainum[++]
Howard University, Washington D.C., 20059, USA
E-mail: pbainum@fac.howard.edu

Space robots and space teleoperators also called telerobots are currently being developed in the USA, Europe, Canada, Russia and Japan for use in the International Space Station (ISS) and in planetary and lunar scientific missions. The robot applications in space missions became very attractive for several reasons.

First of all robot could develop activities that are dangerous and risky for the humans. In addition the use of astronauts for space operations is too costly and involves significant safety risk. The space environment is not natural for humans. Any human activity in space requires designing and testing devices to provide oxygen in space, to provide protection against large temperature variation as well as to provide protection against the space environment pressure and radiation. Also the astronauts must be trained to work in the g-zero or micro gravity environment. Even tasks such as to work while using a space suit require many ours of training. The dressing of a space suit that for many look like a simple task requires hours of work and a second person to help. The robot can replace the man's work in various situations in space. The combination of the human and the robotics work (telerobotics) saves time and reduce the risk of life for humans in space operations. A space robot may be an entire spacecraft or a subsystem of a space vehicle, as for instance the shuttle manipulator robot system (SRMS). The Sputnik, the first artificial satellite launched by the former URSS can be considered as a space robot with the mission of sending radio signal to Earth. Automated orbiters and lenders have explored the Moon, Mars and Venus. Presently space robots are on the Mars

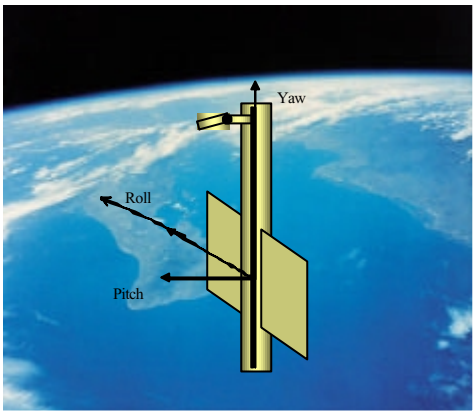

Figure 1 In-Orbit Station Physical Model

[+] Professor and Control Engineer, Space Mechanics and Control Division, INPE, S.J, Campos, S.P., Brazil.

[++] Distinguished Professor of Aerospace Engineering, Dept. of Mechanical Engineering, Howard University, Washington D.C.; Fellow AIAA, Fellow AAS, Member IAA

surface collecting and analyzing rock samples and looking for evidence of water and possible life in the red planet. Examples of automated spacecraft like robots are Mariner, Magellan, Surveyor, Viking, and Veneras. The advent of the large space systems as the space shuttle, space stations, and the power satellite concept gave birth to the space robot manipulator systems design. The design of these manipulators would require taking into account new aspects of the dynamics never considered before for the robot manipulators, such as the operation in the micro gravity environment and the manipulator operation on a mobile (non-inertial) base that always react (based on the action and reaction Newton's law) to the manipulator work of grasping and moving payloads along the mother spacecraft. The space shuttle started a new era in space transportation with its reusability and new features of operation in space. Such operations require the usage of robot manipulators to grasp a spacecraft while it is being repaired in orbit, as it was the case of the successful refurbishment of the Hubble Space Telescope in 1993. The SRMS, or Canadarm, flew for the first time on-board the Space Shuttle Orbiter, Columbia, in 1981. That was the second Shuttle transportation mission[1]. It took nearly seven years for Canada to build the robotic manipulator for the Shuttle transportation missions. Since that time, the SRMS has been used extensively for payload deployment and retrieval. A new generation of space manipulators is planned to operate on-board the International Space Station (ISS), providing services of payload transportation and maneuvering as well as Shuttle berthing and deberthing, etc. Another teleoperation remote manipulator system is the special dexterous manipulator, to provide the ISS with more delicate and dexterous assembly tasks. These robotic manipulators are part of the mobile servicing system of the ISS. The Japanese Experiment Module is also a manipulator system built by Japan, a partner in the development of the ISS. From 1981 to 1992 28 SRMS different missions have been accomplished[2].

The on-orbit teleoperation involves robots manipulating masses that are not negligible as compared with the mass of the mother satellite, or Shuttle. These on-orbit operations present various and difficulties and challenges[3]. Among those difficulties, presented in reference 3, we can include robot path planning, interaction between robot motion and vehicle attitude dynamics and control, and the flexibility of the SRMS. The first difficulty (the robot path planning) differs from the problem for Earth-based manipulators. On the Earth-based manipulators the designer considers the robot mounted on an inertial fixed base. In space the robot is mounted on a mobile base. The mother space vehicle can move as a result of Newton's action and reaction law when the SRMS operates. Reference 3 illustrates these difficulties with the following example: consider the SRMS mounted on a Shuttle of mass *67,000 Kg* that can manipulate a maximum payload of *30,000 Kg*. By commanding the robot to move this load through a distance of 6 m, would cause the Shuttle to have a relative motion of about *1.8 m* (considering both as point masses, for simplicity). The result is an actual motion of only *4.2 m*. The robot would miss its target by *1.8* meters. Let us consider now the time the astronauts consume when they have to operate the SRMS. Approximately one-third of the time that they spend to operate the SRMS is consumed by waiting for vibrations to decay to a required *2-in* level before grasping one object. This means that for every *6* hours of operation of the SRMS during a space flight, the astronauts spend 2 hours waiting for vibrations to decay. The problem of flexibility may become more complicated if we consider that the mother vehicle is a large space structure that

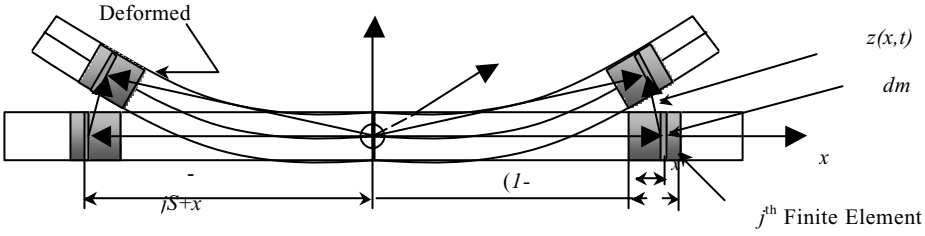

Fig. 2 – j^{th} Finite Elements, Left and Right Side of the Main Bus

also experiences flexible vibrations, in addition to the structural RMS flexibility. We should point out that the manipulator structural flexibility assumption is not a simply theoretical idea. Actually the weight saving is critical for space missions. Because of the expense of launching mass into space, the RMS exhibits significant structural flexibility. Another fact that contributes to this is the size of the manipulator arms. Large workspace requirements require that some of the manipulators be long and thin. New material and special shape designs try to overcome the elasticity problem. However, so far, we cannot avoid having structural flexibility in designing long manipulator arms, such as those built for the space Shuttle and ISS missions. The MRS structural vibration interacts with the attitude control systems. In this paper we analyze this attitude and vibration problem a large space structure containing an RMS. In the next section, we present the physical and mathematical model of this space station as well as its control law formulation.

Mathematical Modeling

The mathematical model is obtained by combining the Finite Element Method (FEM) with the Lagrangian formulation, for generalized and for quasi-coordinates[4],[5] . Then the equations of motion are linearized about the gravity-gradient stabilized nominal local vertical orientation. The linearization procedures follow Kaplan[6], except for the fact that our model is flexible and includes the RMS. The physical model of the space station consists of a long tubular beam (representing the main bus), two tubular beams connected to the main bus and to each other by joints (representing the RMS) and two long solar panels, approximated by thin plates, clamped on the base of the main bus. Figs. 1 and 2 illustrates the physical model.

In order to apply the FEM technique to model the space station, consider Fig. 2, which shows the finite element definition and the vector position of an elemental mass in the finite elements, at the right and the left side of the main bus. We have eliminated any structural rigid body translation. In this case, the system center of mass is constrained to follow the (assumed) circular orbit path and the orbital rate is constant. Observe that these modeling assumptions make the free-free space structure different from the Earth based free-free beam model. In spite of the fact that the station is a free-free structure in space, its rigid body motion is restricted to the attitude degrees-of-freedom (rotational motion about its center of mass). We have used the MATLAB® Symbolic Math Toolbox and its associated FORTRAN representation of symbolic expressions, to obtain the mathematical model and its mathematical expressions in FORTRAN code, respectively. Then the coded part of the model was inserted into the computer routines that we have built to implement the numerical simulations.

The main steps in using the Lagrangian Formulation in conjunction with Finite Elements to obtain the mathematical model for the station are:

- Derive the mass matrix for the finite element *j* of each component of the station system
- Derive the stiffness matrix for the finite element *j* of each component of the station system
- Assemble the mass and the stiffness matrices for the complete system
- Write the Lagrangian function given by *T*-*V*, where *T* and *V* stands for kinetic and potential energy, respectively
- Derive the (external) torques associated with the gravity-gradient
- Use Lagrange's formula for quasi-coordinates and for generalized coordinates to obtain the equations of motion.

Consider now the element of mass *j,* Fig. 2, of the main bus. The position of an elemental mass of the element in the deformed configuration can be written as

$$\{R\}=\begin{Bmatrix}(j-1)s+x\\0\\z_k(x,t)\end{Bmatrix}=\begin{Bmatrix}(j-1)s+x\\0\\\sum_{j=1}^{4}\phi_j(x_k)q_{kj}(t)\end{Bmatrix} \quad (1)$$

$$\{\mathbf{R}\}=\begin{Bmatrix}-js+x\\0\\\sum_{j=1}^{4}\phi_j(x_k)q_{kj}(t)\end{Bmatrix} \quad (2)$$

for the right and the left hand side of the main bus, respectively. The shape functions can be written in matrix form

$$z_k(x_k,t)=[\Phi]\{\mathbf{q}\} \quad (3)$$

For beam elements we can chose this matrix to be

$$[\Phi]=[\phi_1 \quad \phi_2 \quad \phi_3 \quad \phi_4] \quad (4)$$

where the components ϕ_i are, respectively:

$$1-3\frac{x^2}{s^2}+2\frac{x^3}{s^3}\ ,\quad x-2\frac{x^2}{s}+\frac{x^3}{s^2},\quad 3\frac{x^2}{s^2}-2\frac{x^3}{s^3}\ ,\quad -\frac{x^2}{s}+\frac{x^3}{s^2}$$

$$\{\mathbf{q}\}=\begin{Bmatrix}q_1\\q_2\\q_3\\q_4\end{Bmatrix} \quad (5)$$

The derivative of {**R**} with respect to time, *t*, can be written in matrix form as

$$\{\dot{\mathbf{R}}\}=[\tilde{\mathbf{R}}]^T\{\omega\}+[\mathbf{D}]\{\dot{\mathbf{q}}\} \quad (6)$$

where

$$\{\dot{\mathbf{R}}\}=\begin{bmatrix}0&-R_z&R_y\\R_z&0&-R_x\\-R_y&R_x&0\end{bmatrix}^T \quad (7)$$

$$\{\omega\}=\begin{Bmatrix}\omega_x\\\omega_y\\\omega_z\end{Bmatrix} \quad (8)$$

$$[\mathbf{D}]=\begin{bmatrix}\frac{\partial\{\mathbf{R}\}}{\partial q_1}&\frac{\partial\{\mathbf{R}\}}{\partial q_2}&\frac{\partial\{\mathbf{R}\}}{\partial q_3}&\frac{\partial\{\mathbf{R}\}}{\partial q_4}\end{bmatrix} \quad (9)$$

By using these definitions, we can write the kinetic energy for the element *j* of the main bus as:

$$T_j=\frac{1}{2}\int_{m_j}\{\dot{\mathbf{R}}\}^T\{\dot{\mathbf{R}}\}dm_j=\frac{1}{2}\{\omega\}^T\int_{m_j}[\tilde{\mathbf{R}}][\tilde{\mathbf{R}}]^T dm_j\{\omega\}+$$
$$\frac{1}{2}\{\dot{\mathbf{q}}\}^T\int_{m_j}[\mathbf{D}]^T[\mathbf{D}]dm_j\{\dot{\mathbf{q}}\}+\{\omega\}^T\int_{m_j}[\tilde{\mathbf{R}}][\mathbf{D}]dm_j\{\dot{\mathbf{q}}\}$$
$$T_j=\frac{1}{2}\{\omega\}^T[\mathbf{J}_j]\{\omega\}+\frac{1}{2}\{\dot{\mathbf{q}}\}^T[\mathbf{m}_j]\{\dot{\mathbf{q}}\}+\{\omega\}^T[\mathbf{E}_j]\{\dot{\mathbf{q}}\} \quad (10)$$

$$T_m=\sum_{j=1}^{n_{em}}T_j$$

where the matrices [$\mathbf{J}_j$], [$\mathbf{m}_j$], and [$\mathbf{E}_j$] result from the integrals over the mass domain. Similar procedure is done to obtain the kinetic and elastic potential energy, respectively, for the two connected tubes of the robotic manipulator and the thin plates of the solar arrays (See Fig. 3) . The modeling of the solar arrays differs only for the rectangular thin plate elements and the shape functions (instead of the beam shape functions, given by Eq.(4)). So, by doing the same for each part of the space station we can obtain the kinetic energy for the manipulator and the solar arrays. Then, by using the FEM, we assemble the matrices associated with the finite elements of each part of the space station to obtain the total system kinetic

energy, *T*.

We can obtain the elastic potential energy, *U*, by the same approach. This energy can be written as

where the ℓ^2_{xRo}, $\ell^2_{yR_o}$, and $\ell^2_{zR_o}$ are the direction cosines that relate the attitude angles with the orbital reference system of axes. $\mathbf{R}_o$ refers to the vector position of the center of mass of the station with respect to the center of the Earth (see

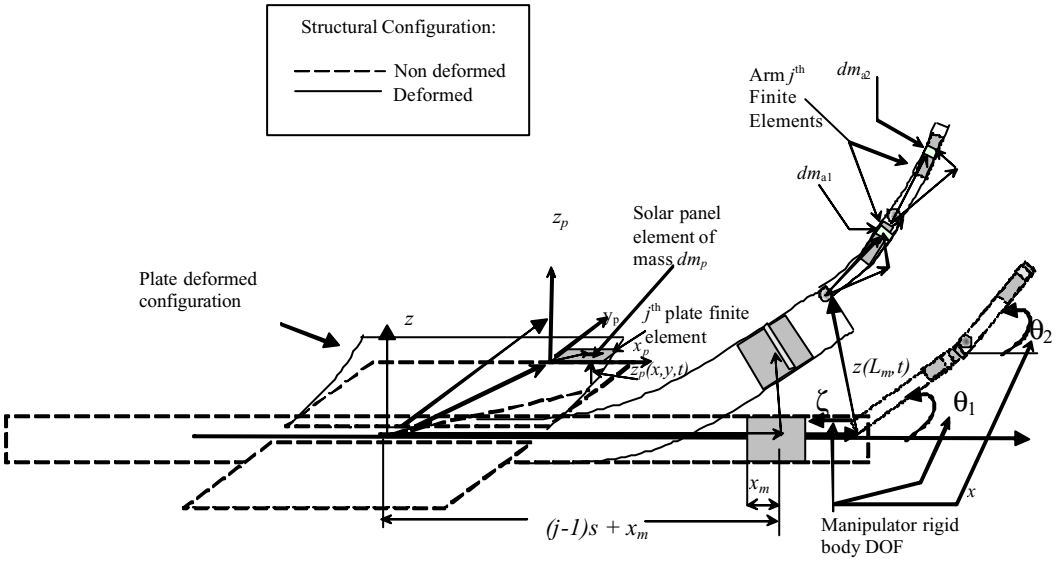

Fig. 3 –Space Station Components -Finite Elements and Elemental Masses (dm_p,dm_{a1}, and dm_{a2}) Position

$$U = \frac{1}{2}\{e\}^{\mathbf{T}}[\mathbf{K}]\{e\}, \qquad \{\mathrm{e}\} = \begin{Bmatrix} \theta_1 \\ \theta_2 \\ \zeta \\ \{\mathbf{q}\} \end{Bmatrix} \qquad (11)$$

where {e} is the vector of the generalized coordinates including the rigid body DOF of the manipulator, θ_1, θ_2, and ζ (translational DOF). $[\mathbf{K}]$ is the structural stiffness matrix. The gravitational potential energy, *Vg*, can be written as

$$V_g = -\frac{\mu_\oplus m_e}{R_o} - \frac{3}{4}\frac{\mu_\oplus m_e}{R_o^3}\left(\ell^2_{xR_o}(I_x + I_z - I_y) + \ell^2_{yR_o}(I_x + I_y - I_z) + \ell^2_{zR_o}(I_y + I_z - I_x) \right) \qquad (12)$$

Fig. 4 for illustration). It should be pointed out here that we have neglected all the elastic displacement contributions to the gravity-gradient. It is a reasonable assumption since the gravity-gradient is of the magnitude of a position in the station to the radius $\mathbf{R}_1$. This is to say that the gravity-gradient is small. The elastic displacement is completely negligible since it is a small value contributing to a yet small value. The expression for the gravitational potential energy does not have to enter into the Lagrangian function. Instead we can derive the gravitational torque by using Eq.(12) so that the torque is computed as an external torque associated with the Euler rotational equations of motion. Note that the Lagrangian function

$$L = T - U \qquad (13)$$

is a function of the generalized coordinates and velocities, e_i, $\dot{e}_i$, and the rotational angular

velocities ω_x, ω_y, and ω_z. The angular velocities are implicit functions of the Euler angles and rates. They cannot be integrated to obtain the corresponding coordinates. In other words ω_x, ω_y, and ω_z are not generalized velocities obtained from the time derivative of the generalized coordinates. To use the Lagrangian formulation to obtain the Euler Equations we use the Lagrangian formula for quasi-coordinates given by

$$\frac{d}{dt}\left\{\frac{\partial T}{\partial \omega}\right\}+[\tilde{\omega}]\left\{\frac{\partial T}{\partial \omega}\right\}=\{\mathbf{M}_o+\mathbf{f}_o\} \qquad (14)$$

where $\mathbf{M}_o$ is the external torque vector, associated with the gravity-gradient torque and $\mathbf{f}_o$ is the control torque vector. $\mathbf{M}_o$ can be obtained through the expression of the gravitational potential energy, V_g. Eq.(14) yields the Euler modified equations of motion accounting for the contribution of elastic acceleration and the accelerations associated with the robot dynamics. By combining the use of the Eq.(14) and the Lagrangian formula for generalized coordinates, $\frac{d}{dt}\left(\frac{\partial L}{d\dot{e}_i}\right)-\frac{\partial L}{de_i}=Q_{e_i}$, we obtain the complete set of equations of motion for the space station as:

$$\begin{Bmatrix}\{\ddot{\Psi}\}\\ \{\ddot{\mathbf{e}}\}\end{Bmatrix}=-\begin{bmatrix}[\mathbf{J}] & [\mathbf{E}]\\ [\mathbf{E}]^T & [\mathbf{m}]\end{bmatrix}^{-1}\left(\begin{bmatrix}[\mathbf{G}] & [\tilde{\Omega}][\mathbf{E}]\\ [\mathbf{0}] & [\mathbf{0}]\end{bmatrix}\begin{Bmatrix}\{\dot{\Psi}\}\\ \{\dot{\mathbf{e}}\}\end{Bmatrix}+\begin{bmatrix}[\mathbf{C}] & [\mathbf{0}]\\ [\mathbf{0}] & [\mathbf{K}]\end{bmatrix}\begin{Bmatrix}\{\Psi\}\\ \{\mathbf{e}\}\end{Bmatrix}-\begin{Bmatrix}\{\mathbf{f}_o\}\\ \{[\mathbf{H}]\{\mathbf{f}\}\}\end{Bmatrix}\right) \qquad (15)$$

The control problem formulation requires the development of the state matrix or plant matrix. In order to obtain this matrix let us define the state vector as

$$\{X_1\}=\begin{Bmatrix}\Psi\\ e\end{Bmatrix} \text{ and } \{\dot{X}_1\}=\{X_2\}=\begin{Bmatrix}\dot{\Psi}\\ \dot{e}\end{Bmatrix}$$

so that we can write the state equation as

$$\begin{Bmatrix}\dot{X}_1\\ \dot{X}_2\end{Bmatrix}=-\begin{bmatrix}[\mathbf{0}] & [\mathbf{I}]\\ [\overline{\mathbf{K}}] & -[\overline{\mathbf{M}}]^{-1}[\overline{\mathbf{G}}]\end{bmatrix}\begin{Bmatrix}X_1\\ X_2\end{Bmatrix}+\begin{bmatrix}[\mathbf{0}] & [\mathbf{0}]\\ [\mathbf{0}] & -[\overline{\mathbf{M}}]^{-1}\end{bmatrix}\begin{Bmatrix}0\\ \overline{u}\end{Bmatrix} \qquad (16)$$

where

$$[\overline{\mathbf{M}}]=-\begin{bmatrix}[\mathbf{J}] & [\mathbf{E}]\\ [\mathbf{E}]^T & [\mathbf{m}]\end{bmatrix} \qquad [\overline{\mathbf{K}}]=\begin{bmatrix}[\mathbf{C}] & [\mathbf{0}]\\ [\mathbf{0}] & [\mathbf{K}]\end{bmatrix}$$

$$[\overline{\mathbf{G}}]=\begin{bmatrix}[\mathbf{G}] & [\tilde{\Omega}][\mathbf{E}]\\ [\mathbf{0}] & [\mathbf{0}]\end{bmatrix} \qquad \{\overline{u}\}=\begin{Bmatrix}\{\mathbf{f}_o\}\\ \{[\mathbf{H}]\{\mathbf{f}\}\}\end{Bmatrix}$$

The last term of Eq.(16) can be rearranged to write the state equation in the classical form:

$$\{\dot{\mathbf{x}}\}=[\mathbf{A}]\{\mathbf{x}\}+[\mathbf{B}]\{\mathbf{u}\} \qquad (17)$$

where $\{\mathbf{x}\}=\begin{Bmatrix}X_1\\ X_2\end{Bmatrix}$

Now that we have written the state equation, we can consider the optimal regulator problem: Given Eq,(17), we need to determine the gain matrix [**F**] for the optimal control vector

$$\{\mathbf{u}\}=-[\mathbf{F}]\{\mathbf{x}\} \qquad (18)$$

so as to minimize the performance index

$$I_c=\int_0^\infty\left(\{\mathbf{x}\}^T[\mathbf{Q}]\{\mathbf{x}\}+\{\mathbf{u}\}^T[\mathbf{R}]\{\mathbf{u}\}\right)dt \qquad (19)$$

where [**B**] is the input matrix, [**Q**] is a positive-definite or positive semi-definite matrix, and [**R**] is a positive-definite matrix. In this formulation we consider that the state is completely observable and accesssible so that the feedback control can be accomplished without estimation. The optimum matrix [**F**] is given by

$$[\mathbf{F}] = [\mathbf{R}]^{-1}[\mathbf{B}]^T[\mathbf{P}] \quad (20)$$

where [**P**] is the Riccati matrix . It is a symmetric positive definite matrix, obtained by solving the algebraic Riccati equation:

$$[\mathbf{A}]^T[\mathbf{P}] + [\mathbf{P}][\mathbf{A}] + [\mathbf{Q}] - [\mathbf{P}][\mathbf{B}][\mathbf{R}]^{-1}[\mathbf{B}]^T[\mathbf{P}] = 0 \quad (21)$$

By substituting Eq.(18) into Eq.(17) we obtain the state equation in terms of the state only, as

$$\{\dot{\mathbf{x}}\} = ([\mathbf{A}] - [\mathbf{B}][\mathbf{F}])\{\mathbf{x}\} \quad (22)$$

The matrix [**A**]-[**B**][**F**] is called the closed-loop matrix. The damping factor associated with the control results from solving the eigenvalue problem of [**A**]-[**B**][**F**]. In the next section we implement the numerical simulations to analyze the space dynamics during the robotic manipulator operation.

Simulations and Results

We have used the MATLAB® to implement the numerical applications for a structure with the following properties and parameters:

Material density = *1769 Kg/m*^{3}
Young's Modulus = *7.3084e10 N/m*^{2}
Main Bus length = *100 m*
Manipulator arms length = *10 m*
Solar panel dimensions = *10 x 10 x 0.003(m)*
Average Main Bus Diameter = *5 m*
Manipulator Arms Diameter=*0.01m*

We have considered first the space station in its normal mode of operation, defined here as

$$\psi_x = \psi_y = \psi_z = \dot{\psi}_x = 0 \pm 0.05^0$$

We have assumed that all the elastic displacements are small (order of 10^{-3} *m*) in this configuration. We start then commanding the arm along the main bus, while the attitude control system (ACS) is turned off. The results are discussed by comparison with the nominal attitude that we have assumed. We show that, for any attitude change, the ACS can be turned on to recover the nominal attitude. We should clarify here that the command of the RMS is not done by the ACS. The LQR technique that we apply here is used to recover the attitude, to damp the structural vibration, and to take the RMS to zero position and rates. By setting appropriate initial conditions, we obtain the time history of the manipulator motion, via integration of the equations of motion of the open-loop system. To simulate the translation of the RMS base, while the control is on, the following strategy is used: we integrate simultaneously the open-loop and the closed-loop systems of equations. The output is compared graphically to show how the time history of both systems differs. Of course, the time history of the system with ACS on shows damping in the overall motion, including the RMS translation. However, the result reflects the time history of the system motion when the control is turned on. The main idea of this approach is to obtain the time history of the open-loop system and then compare the system configuration with the nominal specified settings in attitude and vibration. The result could serve as guidance for missions, which consider operating RMS with the ACS off. In this formulation, we show also that the control law, as we have designed here, can be turned on at any time, to bring the spacecraft to the normal mode of operation.

We have implemented the numerical simulations considering two different cases: one in which the system is gravity-gradient stabilized and the active control is off; and the other in the same situation, with the active control turned on. It is well known that for the gravity-gradient stabilized case the system oscillates about the local vertical, if there is any misalignment with respect to the vertical. The active control is used to damp the misalignments and to maintain the spacecraft within the nominal attitude and rates. As we have a non-rigid system in the sense that we have a mobile RMS and that the space structure is flexible, our attitude control system is used to damp the elastic displacements as well as to control the RMS translational and rotational motions. We assume here that the operation with the control off should not last more than *1* minute. We show that, for the gravity-gradient stabilized case, we can move the RMS

base during that time span without any problem. We show first that we have designed an effective control system capable of recovering the attitude from angles of about 5 degrees and initial elastic displacements of order of $10^{-2}m$, and which is also capable of maintaining the spacecraft within the nominal attitude. To accomplish this goal we have input the following values for the elements of the **[Q]** and **[R]** penalty matrices

$Q(i,i)=10^{7}$, $i = 1$ to 132

$R(i,i)=10^{7}$

except for

$R(2,2)=R(3,3)=R(7,7)=R(8,8)=1.0$

The penalties above are associated with the roll and pitch attitude angles, and the elastic displacement at the left and right hand side of the main bus, respectively. $R(1,1)$ is associated with the yaw attitude angle. $R(4,4)$ to $R(6,6)$ are related to the rotation angles, θ_1 and θ_2, and the translation of the RMS base, ζ, on the space station, respectively. $R(9,9)$ to $R(12,12)$ are associated with the control forces that actuate on the tip of each arm of the manipulator and each tip of the solar arrays. Fig. 5 shows the components of the control vector, $\{\mathbf{u}\}$, along the space station.

The control effort necessary to control pitch and roll is much greater than the control effort necessary to control yaw. The reason is that the yaw axis is the axis of minimum moment of inertia while pitch and roll inertias are of the same order and much bigger. Note that the moment of inertia around the yaw axis involves the square of the main bus radius (about $5\ m$) while the moment of inertia about the roll and pitch axes involves the square of half of the main bus length (about $50\ m$). Because of the great difference between the moments of inertia we avoid giving the same penalties for the control matrix elements associated with yaw, pitch and roll. By giving less penalty to yaw we avoid overdamping in that mode. A very high damping rate would increase the energy expenditure and consequently the cost. By balancing the penalties in the present work, we maintain the same order of transient decay rates in all three attitude angles and guarantee the damping of the elastic displacements. Fig. 6 shows the attitude (yaw, roll, and pitch) time history for the atitude control system, ACS, off. This picture illustrates the oscillatory nature of the gravity-gradient stabilization when there are some misalignments. Fig. 6 shows the case when the misaligment is about 5^0 about all three axes. Fig. 7 shows the results for the the simulation of the same configuration but with the ACS on. In Figs. 8 -11 we show the various results we have obtained for *1* minute operation of the RMS, with and without the ACS actuation. We have assumed a small misalignment (0.05^0) in attitude and a low amplitude for elastic displacement of the main bus and the solar panel tips (order of $10^{-3}m$).

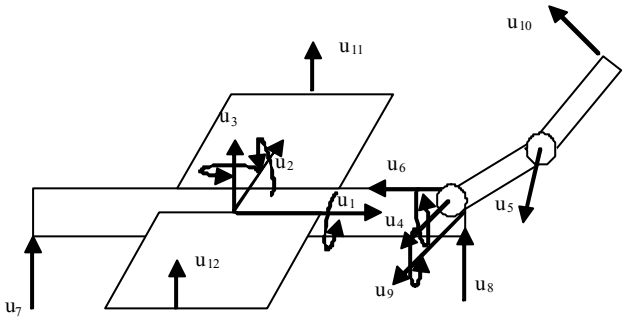

Fig. 5 – Distribution of the Vector $\{\mathbf{u}\}$ Along the Space Station

Anais do 3R Congresso Temático de Dinâmica e Controle da SBMAC
31-maio a 3-junho-2004
UNESP – Campus de Ilha Solteira

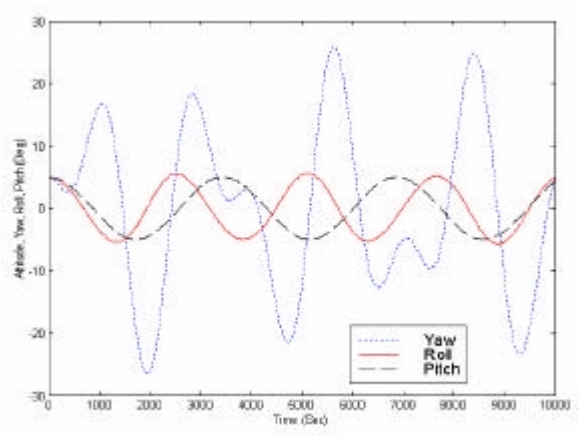

Fig. 6–Attitude Time History, ACS Off

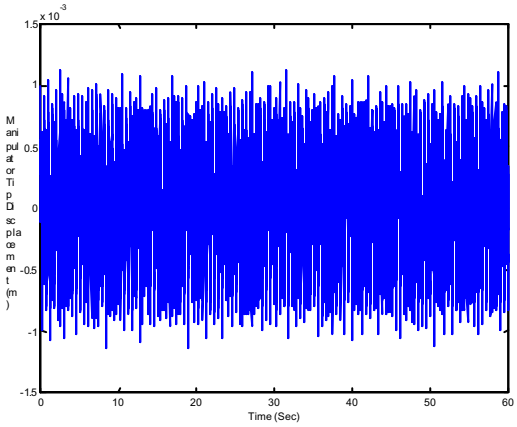

Fig. 9 – RMS Displacement ACS Off

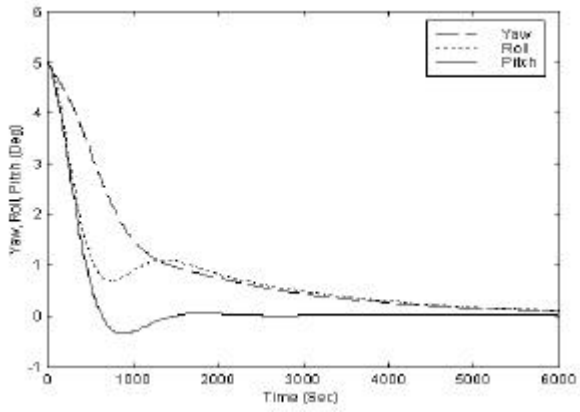

Fig. 7–Attitude Time History, ACS On

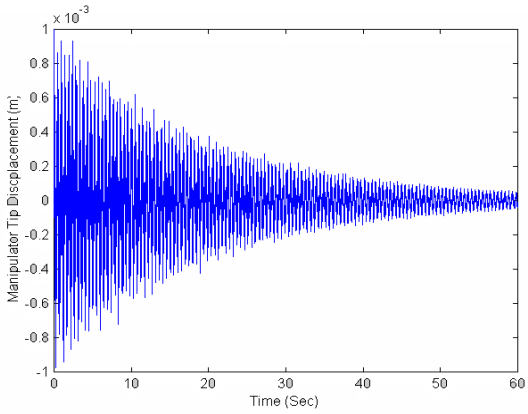

Fig. 10 – RMS Tip Displacement, ACS On

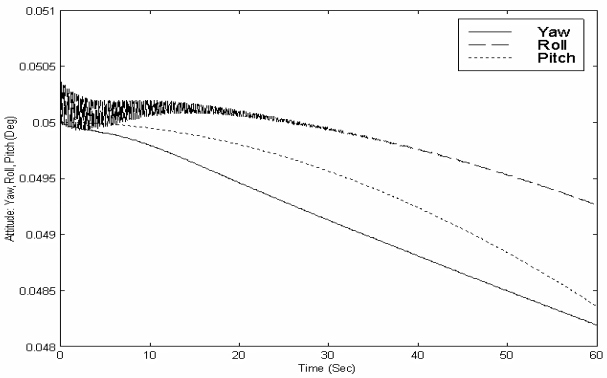

Fig. 8–Attitude Time History, ACS On

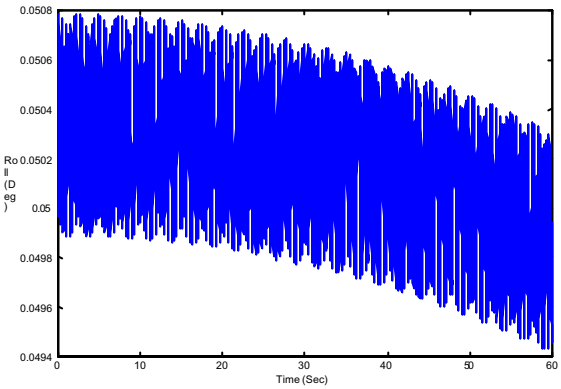

Fig. 11 –Roll Time History – ACS Off

All the results for this case show that the RMS base motion does not significantly disturb the attitude.

Conclusion

We have developed the model for a space station in low Earth orbit, for the gravity-gradient stabilized case, to analyze the attitude behavior during maneuvers with the RMS. We have formulated the active attitude control for the structure by using the LQR technique. The results show the attitude control damps the oscillations in attitude as well as the vibration. The results show also that for short duration of RMS maneuvers, the attitude does not change significantly.

References

[1]. Nguyen, Phung K. and Hughes, Peter C.; Teleoperation: From the Space Shuttle to the Space Station, in *Teleoperation and Robotics in Space*, Edited by Steven B. Skaar and Carl F. Ruoff, Progress in Astronautics and Aeronautics, A. Richard Seebass Editor-in-Chief, Vol. 161, 1994, Chapter 14, pp. 353-410

[2].Brimley, W., Brown, D., and Cox, B.; Overview of the International Robot Design for Space Station Freedom, in *Teleoperation and Robotics in Space*, Edited by Steven B. Skaar and Carl F. Ruoff, Progress in Astronautics and Aeronautics, A. Richard Seebass Editor-in-Chief, Vol. 161, 1994, Chapter 15, pp. 411-442

[3]. Longman, Richard W.; Tutorial Overview of the Dynamics and Control of Satellite-Mounted Robots, in *Teleoperation and Robotics in Space*, Edited by Steven B. Skaar and Carl F. Ruoff, Progress in Astronautics and, A. Richard Seebass Editor-in-Chief, Vol. 161, 1994, Chapter 10, pp. 237-258

[4] Meirovitch, L. *Elements of Vibration Analysis*, McGraw-Hill, Inc, 1975, Chapter 8, pp. 286-323

[5] Meirovitch, L. *Methods of Analytical Dynamics*, McGraw-Hill , Inc., 1970, Chapter 4, pp. 157-160

[6] Kaplan, Marshall H.; *Modern Spacecraft Dynamics & Control*, John Wiley & Sons, 1976, Chapter 5, pp.199-200